Reynolds Number Dependence of Bearing Performance

E. Kim[1]

ABSTRACT: Based on the full Navier-Stokes solutions, the thermohydrodynamic performance of a long journal bearing is investigated. A numerical method based on Galerkin's procedure and B-spline test functions has been presented for solving two-dimensional problems involving fluid flow and heat transfer. For numerical stability the artificial compressibility is employed to the conservation of mass. The discretized algebraic equations are solved by Newton's method. Effects of varying the speed of an inner cylinder to load carrying capacity are investigated. The results indicated that the increase of the speed of an inner cylinder has a significant effect on the temperature profile and ultimately on the performance.

INTRODUCTION

The essence of classical bearing theory which provides the mathematical theory of lubrication, is the recognition that the problem has two length scales: the thickness of the film and its lateral dimension [1]. In classical bearing analysis, the bearing performance is predicted on the assumption that the viscosity of the fluid is constant and uniform over the fluid film and that fluid inertia is negligible. These assumptions work well for small, low speed bearings running on petroleum oil fluids, and in such cases the predictions of classical theory are in essential agreement with experiments. However, as the system increases its speed, this assumption is no longer correct [2]. To correct this problem, several investigators have investigated the bearing performance including fluid inertia and heat transfer, respectively. The effect of inertia is estimated from a first-order perturbation solution [3, 4], integral relations [5]. These authors showed that the contribution from the inertia film forces to the load carrying capacity and the dynamic reaction forces of journal bearings is quite small. With the full Navier-Stokes equations keeping the temporal terms for a plane slider bearing, and using a body fitted coordinate system, Sestieri and Piva [6] analyzed the influence of the inertial forces in steady and unsteady lubrication films. Hashimoto [7] investigated the effects of fluid inertia on the performance characteristics of bearings. He derived the momentum and continuity equations including the full inertia terms throughout the film thickness. Then he applied a numerical technique combining the control volume integration and the Newton method to solve equations. It is concluded that the fluid inertia forces have significant effects on the

[1] School of Mechanical Engineering, Pusan National University, Pusan, 609-735 KOREA

static characteristics of the bearings such as the load carrying capacity and the pressure. However, Hashimoto's analysis is based on the assumption that the shear stress is constant across the film. This assumption is indefensible, and so the final conclusion is strongly suspect. Andres, Szeri [8], and Dai et al. [9] solved the Navier-Stokes equations using Galerkin's method for long cylinders. Dai et al. [9] concluded that in long bearings, fluid inertia has negligible influence on bearing load capacity over the whole laminar range of bearing operations, but that bearing stiffness increases linearly with the Reynolds number. The fluid temperature varies significantly as a result of viscous heat dissipation in the fluid film and heat transfer to the surroundings, and consequently effects to the bearing performance. Cope [10], Dowson, Hudson [11], Suganami, Szeri [12], Ezzat, Rohde [13], and Boncompain et al. [14], using approximate equations, showed that thermal effects play a significant role in determining the performance of journal bearings. Most of the results described in this section are solved by approximate equations. Some authors have made efforts to solve the exact equations directly instead of using the approximate method, following different linearization approaches. On the other hand, in this paper the exact equations will be used to obtain an accurate assessment of the effects.

ANALYSIS

A bipolar coordinate system in the representation of the flow field between long, rotating eccentric cylinders, and cylindrical polar coordinates to analyze heatflow in the bearing are employed. The details of the geometry are shown in Fig. 1. The nondimensional governing equations for the fluid flow are

$$\rho \boldsymbol{V}\cdot\nabla\boldsymbol{V} = -\nabla P - \mu\nabla\times(\nabla\times\boldsymbol{V}) + 2(\nabla\mu)\cdot(\nabla\boldsymbol{V}) + (\nabla\mu)\times(\nabla\times\boldsymbol{V}) \tag{1}$$

$$\nabla\cdot\boldsymbol{V} = 0 \tag{2}$$

$$\rho c_P \boldsymbol{V}\cdot\nabla T = k\nabla^2 T + \mu\Phi \tag{3}$$

and for the bearing is

$$\nabla^2 T_b = 0. \tag{4}$$

To nondimensionalize equations (1)-(4), the following dimensionless variables are used:

$$x = \Delta(\alpha - \alpha_1),\ y = \frac{\beta}{2\pi},\ \Delta = \frac{1}{\alpha_2 - \alpha_1},\ h = \frac{H}{a}, \tag{5}$$

$$\{u,v\} = \frac{\sinh|\alpha_1|}{r_1\omega}\{U,V\},\ p = \frac{P}{\rho u_*^2},\ T = \frac{\overline{T}}{T_*},\ \mu = \frac{\overline{\mu}}{\mu_*}.$$

The dimensionless boundary conditions are

$$u(0,y) = 0,\ v(0,y) = \sinh|\alpha_1|,\ u(1,y) = v(1,y) = 0 \tag{6}$$

$$T(0,y)=T_s \qquad T+\Gamma(y)(\cosh\alpha_2-\cos\beta)\frac{\partial T(x,y)}{\partial x}\bigg|_{x=1}=1 \tag{7}$$

$$\frac{\partial\varphi^{(n)}}{\partial y^n}(x,0)=\frac{\partial\varphi^{(n)}}{\partial y^n}(x,1) \qquad \begin{matrix} n=0,1,2,\ldots \\ \varphi=u,v,p,T \end{matrix} \tag{8}$$

In the above equations, the non-dimensional parameters are defined by

$$R=\frac{\rho r_1\omega c}{\mu_*}, \qquad \mathrm{Pr}=\frac{\mu_* c_p}{k}, \qquad E=\frac{(r_1\omega)^2}{c_p T_*}\left(\frac{r_1}{a}\right)^2. \tag{9}$$

Here R is the Reynolds number, Pr is the Prandtl number, and E is the Eckert number and T_* is the reference (shaft) temperature. The governing equations (1)-(4) are solved by Galerkin' method, employing B-spline basis functions. This scheme has already been employed for eccentric cylinder flows by Dai, Dong & Szeri [9] in the isothermal case and by Dai, Dong & Szeri [15] in the non-isothermal, constant wall temperature case. In these instances the pressure was eliminated either by cross-differentiation or by algebraic means, making for a complicated analysis. Here we simplify the task by solving directly for the primitive variables $\{u,v,p,T,T_b\}$. However, for equal interpolation of velocity and pressure the Galerkin mixed formulation of the steady state Navier-Stokes problem yields a singular system. To circumvent the Babushka-Brezzi stability criteria [16], Zinekiewicz & Wu [17] adjoined the artificial compressibility formulation of the equation of mass conservation to the time-asymptotic form of the Navier-Stokes equations.

Thus, the conservation equations for momentum and mass in their unsteady non-dimensional form are as follows:

$$\frac{\partial u}{\partial t}=f^{(1)}(u,v,p) \tag{10}$$

$$\frac{\partial v}{\partial t}=f^{(2)}(u,v,p) \tag{11}$$

$$\frac{1}{c^2}\frac{\partial p}{\partial t}+div\mathbf{v}=0. \tag{12}$$

Time-discretize (12) as

$$\frac{p^{(n+1)}-p^{(n)}}{c^2\Delta t}=-div\mathbf{v}^{(n+\frac{1}{2})} \tag{13}$$

On substituting for the velocity from the time-discretized momentum equations

$$\frac{p^{(n+1)}-p^{(n)}}{c^2\Delta t}=-div\mathbf{v}^{(n)}-\frac{\Delta t}{2}div(f^{(1)},f^{(2)})\Big|_n. \tag{14}$$

Steady state is characterized by $\partial u/\partial t=0$, $\partial v/\partial t=0$ in equations (10, 11) and by $p^{(n+\frac{1}{2})}=p^{(n)}$ in equation (14). In consequence, the following systems of equations for the steady state problem are solved:

$$f^{(1)}(u,v,p)=0 \tag{15}$$

$$f^{(2)}(u,v,p)=0 \tag{16}$$

$$div\mathbf{v}+\gamma div(f^{(1)},f^{(2)})=0 \tag{17}$$

Here γ is a suitably small number (order 10^{-9}). The system obtained in this manner is non-singular.

NUMERICAL RESULTS

The overall numerical procedure iterates between the nonlinear system (15)-(17), representing the conservation equations for linear momentum and mass and the linear system (3,4), symbolizing the conservation of energy in both the fluid film and the outer cylinder. In each step of the iteration the viscosity field is updated. First, initial values such as velocities, variable viscosity, and temperature are assumed. Then, the unknown values from equations (15)-(17) using the initial values can be calculated. Considering the resulting velocities and viscosity profiles, then the temperature distribution directly can be calculated. The whole system iterates until this temperature distribution converges to a certain limit.

To investigate bearing performance, the following two non-dimensional parameters are considered: (i) the Reynolds number R; (ii) the Eckert number E. These two non-dimensional groups are independent parameters in the analysis. In this work, two cases are presented: (a) the dissipation effects, and, separately, on inertia effects; (b) the effects of heat dissipation with the full Navier-Stokes equations in a primitive formulation. Figure 2, for both cases, shows the non-dimensional force for both Sommerfeld and Gumbel boundary conditions in the laminar regime. In the figure the eccentricity ratio is 0.5, but at other eccentricities the results are similar. For the case (a) in Fig. 2, the load carrying capacity *f* is unaffected by changes in the Reynolds number *R* (see Kim and Szeri [18] in detail). For the case (b), the Reynolds number and the Eckert number are related as E=constant $\times R^2$ for constant eccentricity ratio (i.e., constant *a*) and fixed values of the reference thermodynamic quantities. In the result of the case (b) the Eckert number is not shown, because the Eckert number can be obtained by the given the Reynolds number using the equation E=constant $\times R^2$. The non-dimensional force for the case (b) is a strong function of the Eckert number. This means that the change in load capacity is due to changing E. The case (b), thus, is only presented in the following results. Figure 3 shows the temperature distribution at increasing values of the Eckert number, E, which means the increase of the Reynolds number. Though the thickness of the fluid film is $O(10^{-3})$, the range for the x-direction is [0,1]. This gives the distorted view of the temperature distribution in the fluid film. In the figure, it can be seen that the maximum temperature occurs about the middle section of the film. On increasing the Eckert number to E=4.4×10^{-4}, the temperature profile varies moderately. In the present model, the means of cooling the bearing is by

the Newtonian cooling to the ambient. Figure 4 shows the maximum temperature against the Eckert number. It is noted that the maximum temperatures increase when the Eckert number increases. A change in the maximum lubricant temperature of 224% between $E=1.2\times10^{-4}$ and $E=4.4\times10^{-4}$ was noted. Figure 5a, 5b show the stiffness coefficients for both Sommerfeld boundary condition and Gumbel boundary conditions. With the Sommerfeld condition the mixed components of the stiffness matrix are strongly changed and the diagonal components increase linearly with the Eckert number. With the Gumbel condition, all the matrix components decrease linearly, while the another one, K_{xy}, changes steeply. Solutions are obtained here under Sommerfeld and Gumbel pressure boundary conditions. It has not, as yet, been able to implement the physically more correct Swift-Stieber boundary conditions. This is a weakness of the present analysis, as there is evidence that lubricant inertia stretches the lubricant film [19] by moving the cavitation boundary downstream.

REFERENCES

1. O. Reynolds, Philo. Trans. Roy. Soc., **117**, 157-234 (1886)
2. A. Z. Szeri, Tribology, New York (1980)
3. E. Reinhardt and J. W. Lund, J. Lub. Tech., **97**, 159-167 (1975)
4. A. F. Jones and S. D. R. Wilson, J. Lub. Tech. **97**, 101-104 (1974)
5. V. N. Constantinescu, J. Lub. Tech., **92**, 473-481 (1970)
6. A. Sestieri and R. Piva, J. of Lub. Tech., **104**, 180-186 (1982)
7. H. Hashimoto, J. of Tribology, **111**, 406-412 (1989)
8. L. A. San Andres and A. Z. Szeri, J. Appl. Mech., **51**, 869-878
9. R. X. Dai, Q. Dong and A. Z. Szeri, J. of Tribology, 91-Trib-13, 1-12
10. W. F. Cope, Proc. Roy. Soc., Series A, **197**, 201-217 (1949)
11. D. Dowson and J. Hudson, Inst. Mech. Engrg. Lub., Papers 4 and 5. (1963)
12. T. Suganami and A. Z. Szeri, J. of Tribology, **101**, 21-27 (1979)
13. H. Ezzat and S. Rohde, J. of Lub. Tech., **95**, 298-307 (1973)
14. R. Boncompain, M. Fillon and J. Frene, J. of Tribology, **108**, 219-224 (1986)
15. R. X. Dai, Q. Dong and A. Z. Szeri, J. of Tribology **27**, 367-389 (1992)
16. I. Babuska, Numer. Math., **16**, 322 (1971)
17. O. C. Zienkiewicz and J. Wu, Int. J. Numer. Meth. Eng., **32**, 1189 (1991)
18. E. Kim and A. Z. Szeri, J. of Tribology, **119**, 76-84 (1997)
19. H. You and S. S. Lu, J. of Tribology, **109**, 86 (1987)

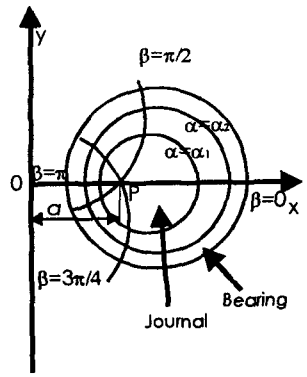

Fig. 1 Coordinate Systems

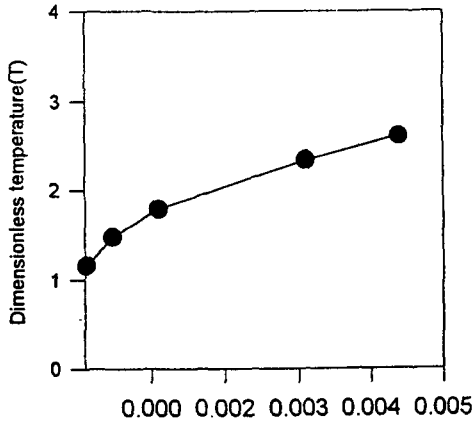

Fig. 4 variation of maximum temperature

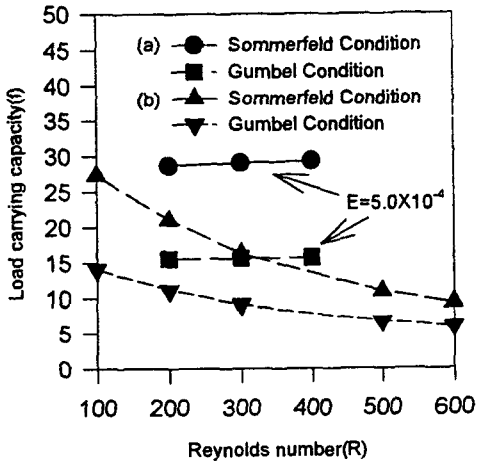

Fig. 2 Variation of load carrying capacity(c/r=0.002, ε=0.5,

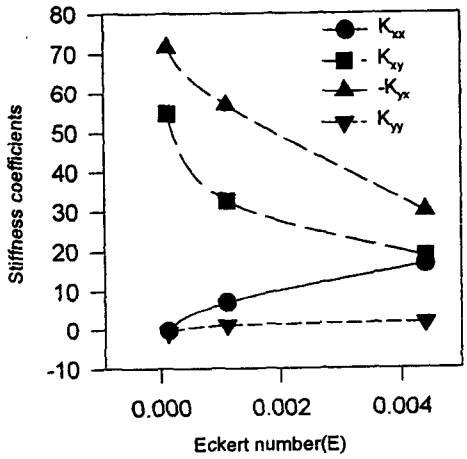

Fig. 5a Variation of stiffness matrix
(Sommerfeld boundary condition, ε=0.5)

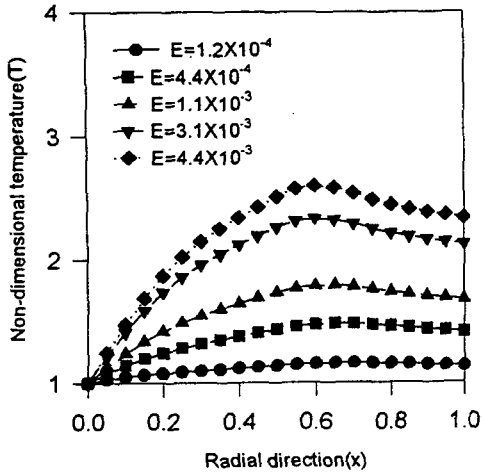

Fig. 3 Radial temperature profile at maximum gap(y=0)
(c/r=0.002,ε=0.5)

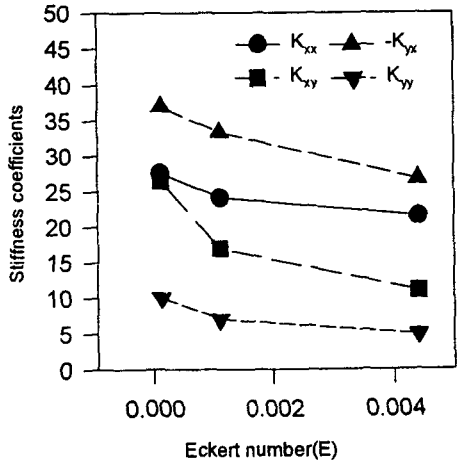

Fig. 5b Variation of stiffness matrix
(Gumbel boundary condition, ε=0.5)